ACS APPLIED MATERIALS & INTERFACES

www.acsami.org

Research Article

Redox-Unlockable Nanoparticle-Based MST1 Delivery System to Attenuate Hepatic Steatosis via the AMPK/SREBP-1c Signaling Axis

Yuhan Li,[#] Jing-Jun Nie,[#] Yuhui Yang,[#] Jianning Li, Jiarui Li, Xianxian Wu, Xing Liu, Da-Fu Chen, Zhiwei Yang,[*] Fu-Jian Xu,[*] and Yi Yang[*]

Cite This: *ACS Appl. Mater. Interfaces* 2022, 14, 34328−34341

Read Online

ACCESS | Metrics & More | Article Recommendations | Supporting Information

ABSTRACT: To date, few effective treatments have been licensed for nonalcoholic fatty liver disease (NAFLD), which a kind of chronic liver disease. Mammalian sterile 20-like kinase 1 (MST1) is reported to be involved in the development of NAFLD. Thus, we evaluated the suitability of a redox-unlockable polymeric nanoparticle Hep@PGEA vector to deliver MST1 or siMST1 (HCP/MST1 or HCP/siMST1) for NAFLD therapy. The Hep@PGEA vector can efficiently deliver the condensed functional nucleic acids MST1 or siMST1 into NAFLD-affected mouse liver to upregulate or downregulate MST1 expression. The HCP/MST1 complexes significantly improved liver insulin resistance sensitivity and reduced liver damage and lipid accumulation by the AMPK/SREBP-1c pathway without significant adverse events. Instead, HCP/siMST1 delivery exacerbates the NAFLD. The analysis of NAFLD patient samples further clarified the role of MST1 in the development of hepatic steatosis in patients with NAFLD. The MST1-based gene intervention is of considerable potential for clinical NAFLD therapy, and the Hep@PGEA vector provides a promising option for NAFLD gene therapy.

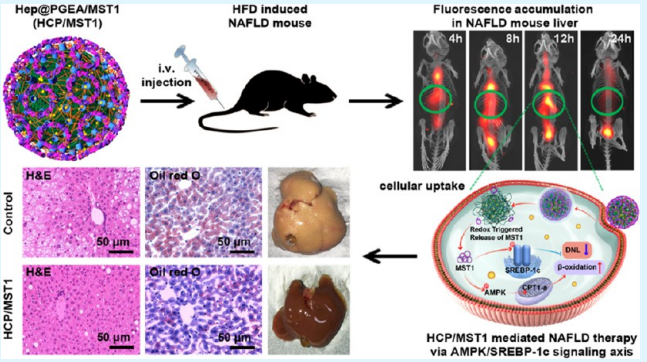

KEYWORDS: *nonalcoholic fatty liver disease (NAFLD), gene therapy, redox-unlockable, self-accelerating release, AMPK/SREBP-1c signaling axis*

1. INTRODUCTION

Nonalcoholic fatty liver disease (NAFLD) is a complex liver disease with abnormal increase of liver lipids and no secondary reasons, such as drugs, significant alcohol intake, or certain genetic conditions.[1] As a heterogeneous disorder, patients with NALFD may progress to nonalcoholic steatohepatitis and further causes liver cirrhosis and liver cancer.[2−4] The global incidence rate of NAFLD is also rising steadily with the rapid increase of obesity, which leads to a significant economic and healthcare burden.[5−7] However, the treatments for NAFLD are still limited, and there is no widely recognized and accepted drug treatment method.[3,8] Thus, the development of effective targeted therapy is an urgent requirement. Pathogenesis of NAFLD is the common influence of various factors such as environment, metabolism, and genetics.[9,10] Several research studies report that in patients with insulin resistance (IR), more free fatty acids are released and these promote de novo lipogenesis (DNL) in the liver, ultimately augmenting the progression of NAFLD.[11−13] We have reported earlier that high-fat diet (HFD)-induced liver energy signal dysfunction is a key mechanism in the liver IR and lipid accumulation associated with NAFLD.[14,15] We also found that mammalian sterile 20-like kinase 1 (MST1), a core member of the Hippo signaling pathway, has great significance in the regulation of lipid metabolism of NAFLD.

Mammalian sterile 20-like kinase 1 (MST1) is a highly conservative serine/threonine kinase, which produces a vital regulatory role in many physiological processes such as cell proliferation and differentiation, cell death and autophagy, and immune response.[16−18] Studies have demonstrated that MST1 can regulate the lipid disorders of the liver by targeting the Sirt1 ubiquitination and ROS production.[19−21] In our previous study, liver-specific MST1 deletion results in liver lipid accumulation by inhibiting AMP-activated protein kinase (AMPK) phosphorylation and carnitine palmitoyltransferase-1alpha (CPT-1α) expression and increasing fatty acid synthase (FAS).[15] Previous studies have also indicated that MST1 considerably reduced lipid accumulation in NAFLD mice liver by reducing DNL and accelerating fatty acid oxidation.[15] Based

Received: April 4, 2022
Accepted: July 11, 2022
Published: July 20, 2022

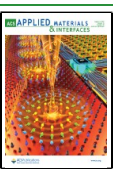

https://doi.org/10.1021/acsami.2c05889
ACS Appl. Mater. Interfaces 2022, 14, 34328−34341

Scheme 1. Schematic Diagram Illustrates the Redox-Unlockable Hep@PGEA Vector-Mediated MST1 or siMST1 Delivery for the Gene Intervention of NAFLD

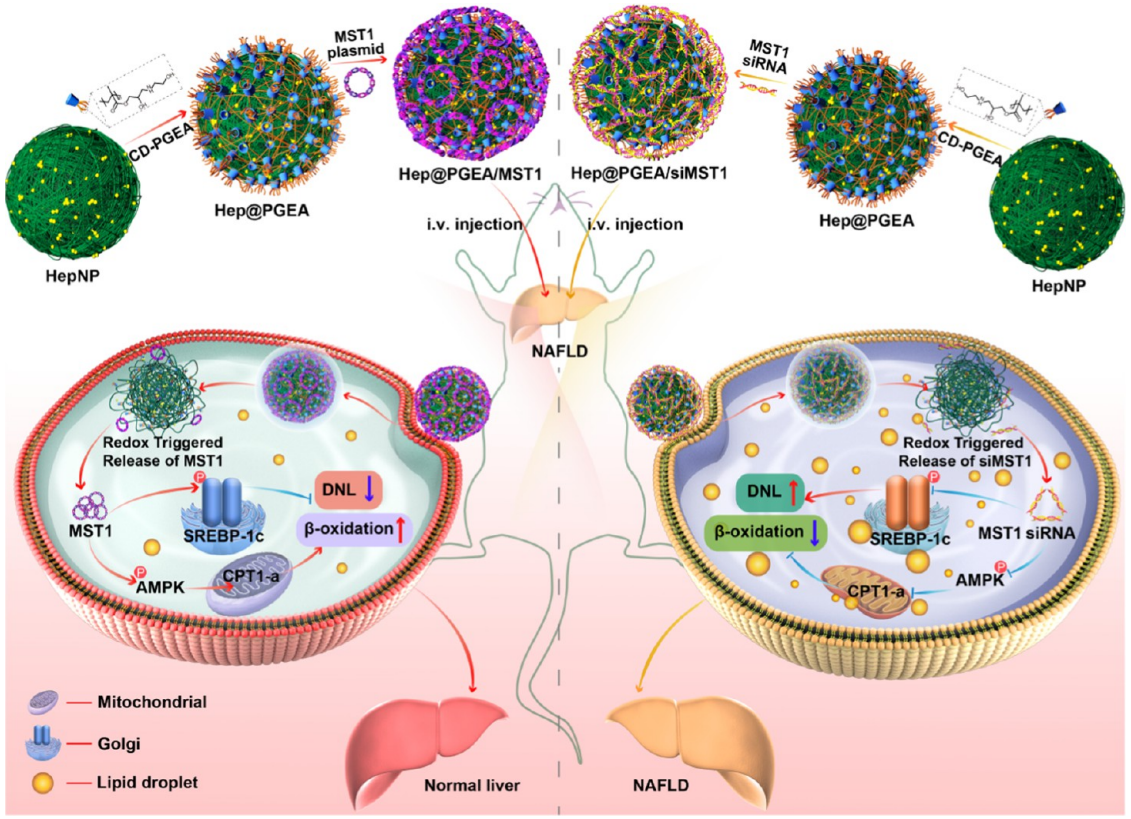

on the above research studies, we hypothesize that MST1 might be a promising target for NAFLD therapy.

Vectors play an important role in determining the effectiveness of gene therapy for their involvements in delivering, protecting, and releasing functional nucleic acids despite various obstacles, such as the rapid degradation of naked nucleic acids in serum and the repulsion of the negatively charged cell membrane to the negative charge of the nucleic acids.[22] As a class of high potential vectors, polycations have attracted considerable attention. Of particular interest are ethanolamine (EA)-modified poly(glycidyl methacrylate) (PGEA) vectors with abundant hydroxyl groups for long circulation.[23] Recently, we developed an unlockable heparin polysaccharide-based PGEA polycation vector (Hep@PGEA) that is capable of responding to the reductants in cells (such as glutathione [GSH]) to accelerate the release of delivered nucleic acids. The complexes performed well for both cardiovascular disease and cancer as gene vectors for either RNA or DNA.[22,24] Owing to the obvious accumulation of the Hep@PGEA-based delivery system in the liver area and high GSH production,[22] we assumed that the Hep@PGEA vector may also prove efficient in delivering MST1 for NAFLD therapy.

The Hep@PGEA vector is composed of a PGEA polycation shell that has abundant hydroxyl groups and a disulfide cross-linked heparin core that can accelerate the release of condensed nucleic acids in PGEA shells after they are unlocked in response to the reductants in the cells. The Hep@PGEA vector shows high gene delivery efficiency and great biocompatibility with different cell lines. It has also been proven to be an excellent delivery vector for the treatment of different diseases.[22−24] Here, we proved the potential of the Hep@PGEA vector in delivering MST1 (HCP/MST1) or siMST1 (HCP/siMST1) for upregulating or downregulating the MST1 protein levels (Scheme 1). The HCP/siMST1 delivery system was shown to accelerate liver fat production by activating sterol regulatory element-binding protein-1c (SREBP-1c), while the overexpression of MST1 mediated by the HCP/MST1 delivery system successfully inhibited hepatic steatosis and maintained lipid homeostasis in NAFLD mice by acting on the AMPK/SREBP-1c signaling axis (Scheme 1). Analysis of clinical NAFLD samples further confirmed the potential of MST1 as an intervention for the treatment of NAFLD. This research supplies an appropriate strategy in the treatment of NAFLD with a Hep@PGEA-based MST1 gene intervention system.

2. RESULTS

2.1. Preparation and Characterization of Hep@PGEA Vector. We first prepared and characterized the Hep@PGEA vector with a negatively charged heparin core that was cross-linked by redox-sensitive disulfide bonds. The particle size of the obtained Hep@PGEA vector was ∼180 nm and the surface determined by the ζ-potential was ∼25 mV (Figure 1a). The condensing ability of the Hep@PGEA vector to MST1 plasmid was subsequently evaluated via an electrophoretic mobility retardation assay. The Hep@PGEA vector effectively condensed the MST1 plasmid at an N/P ratio of 2 (Figure 1b). The particle sizes and ζ-potentials of the complexes decreased with the increase in N/P ratios and then remained nearly constant (Figure 1a).

https://doi.org/10.1021/acsami.2c05889
ACS Appl. Mater. Interfaces 2022, 14, 34328−34341

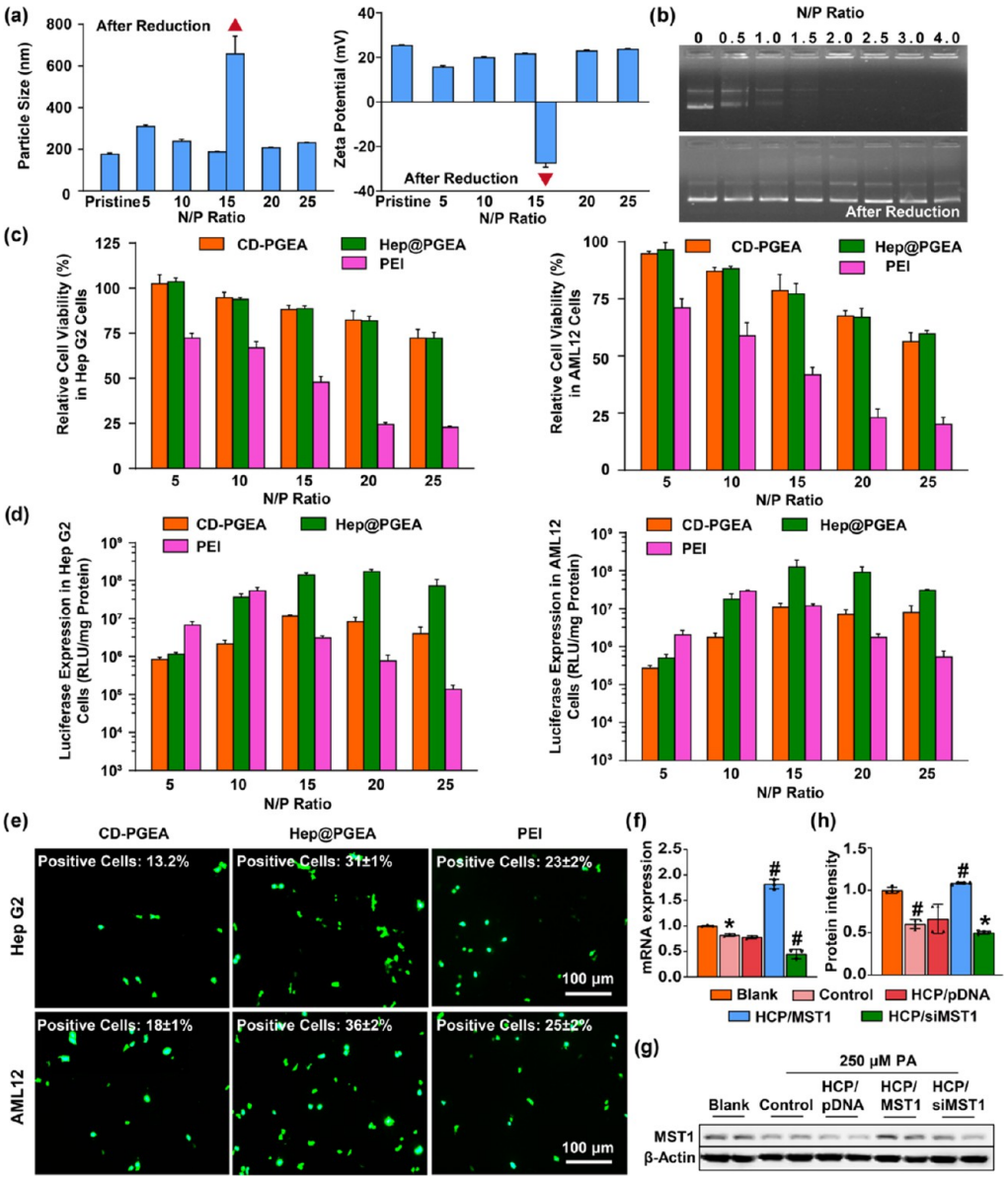

Figure 1. Biophysical properties of the Hep@PGEA vector and gene expression assays in vitro. (a) Particle sizes and ζ-potentials of the Hep@PGEA complexes with or without condensing the MST1 plasmid. (b) Electrophoretic mobility retardation assays mediated by Hep@PGEA for delivering the MST1 plasmid before and after reduction at various N/P ratios. (c–e) Cytotoxicity, luciferase expression, and green fluorescent protein (GFP) expression in HepG2 and AML-12 cell lines mediated by different vectors. (f) mRNA level of MST1 with various treatments. (g, h) MST1 protein levels with various treatments ($n = 4$, $^*p < 0.05$, $\#p < 0.01$; control vs blank, HCP/MST1 vs HCP/pDNA, HCP/siMST1 vs HCP/pDNA; pDNA, negative control plasmid; MST1, functional plasmid-encoding MST1 protein; siMST1, functional plasmid-encoding siRNA of MST1; CD-PGEA, β-CD based cationic PGEA polymer; PEI, M_w ~25 kDa).

The negative core of the Hep@PGEA vector was cross-linked by redox-sensitive disulfides and the vector can be unlocked by reductants in cells like GSH. The unlocked highly negative charged free heparin competitively interacted with a positively charged CD-PGEA shell and accelerated the release of condensed plasmids in the shell, which finally results in the redox-responsive release of condensed plasmids. The reductant (10 mmol/L GSH) was added to evaluate the ability of the Hep@PGEA vector for the self-accelerating release of the MST1 plasmid. Hep@PGEA released the condensed MST1 plasmid while it was exposed to reductant (Figure 1b). The particle size of the HCP/MST1 complexes (Hep@PGEA/MST1 complexes, the Hep@PGEA vector condensed with plasmid-encoding MST1 protein) increased from 180 to 660 nm (N/P = 15) and the ζ-potential changed from positive to negative (from 25 to −27 mV, N/P = 15; Figure 1a).

2.2. Hep@PGEA Vector is a Successful Gene Vector for Lliver-Related Cells. The cytotoxicity of the HCP/pDNA complexes (Hep@PGEA/pDNA complexes, the Hep@PGEA vector condensed with negative control plasmid) at various N/P ratios was evaluated via MTT assay in HepG2 and AML-12 cell lines (Figures 1c and S1). In comparison with the PEI/pDNA complexes at the same N/P ratios, HCP/pDNA and CD-PGEA/pDNA showed higher cell viability, especially when the administrated concentration was high (Figure S1).

Transfection efficiency of Hep@PGEA was assessed by delivering pDNA (Figure 1d). PEI/pDNA and CD-PGEA/pDNA complexes mediated transfection efficiencies were also

https://doi.org/10.1021/acsami.2c05889
ACS Appl. Mater. Interfaces 2022, 14, 34328−34341

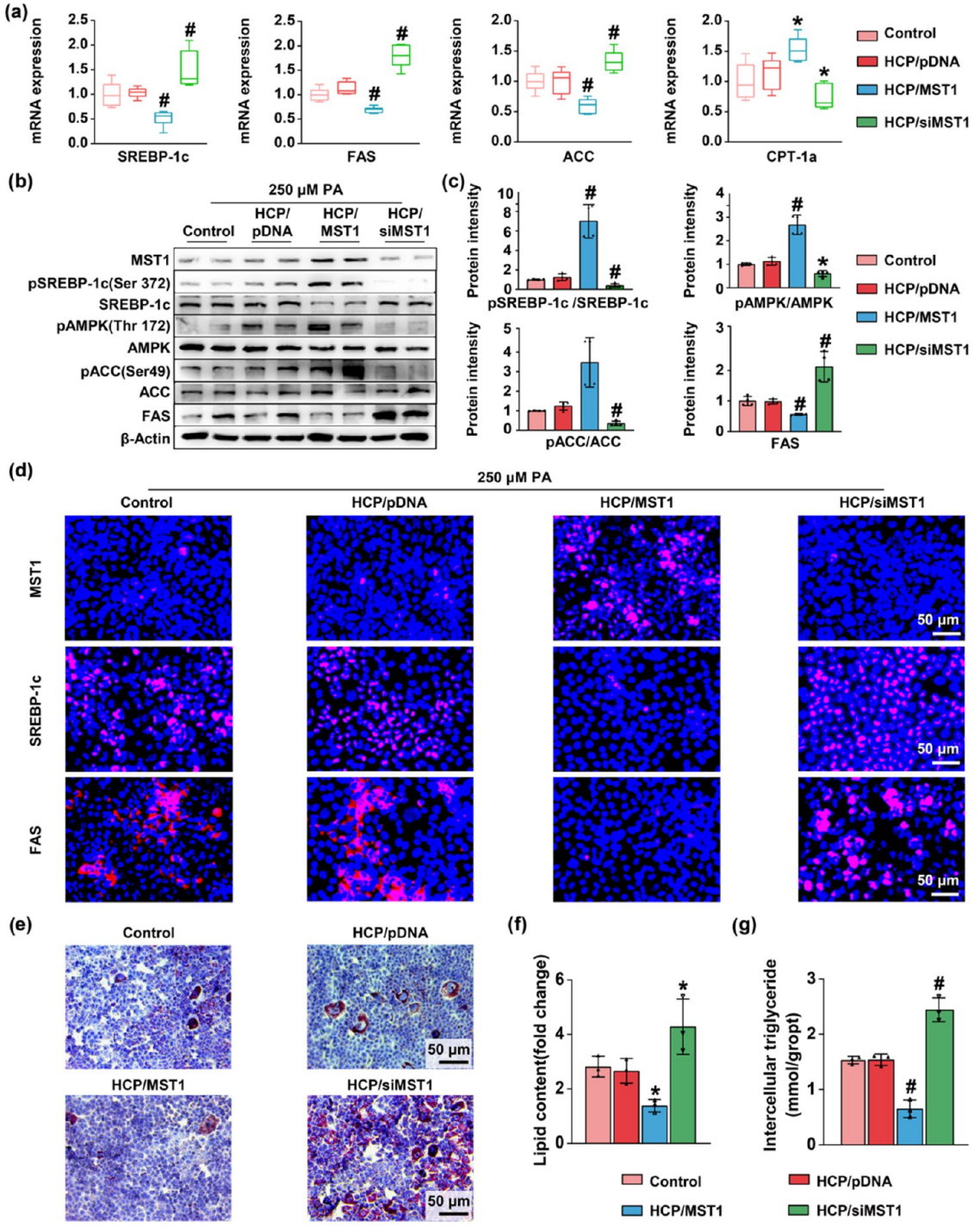

Figure 2. HCP/MST1 and HCP/siMST1 regulate lipid accumulation via the AMPK/SREBP-1c signaling axis in AML-12 cells in the presence of 250 μM PA. (a) mRNA expression of lipogenic genes with different treatments. (b, c) Lipogenic protein levels in different groups. (d) Immunofluorescence analysis for MST1 (red), SREBP-1c (red) and FAS (red). (e, f) Cellular lipid accumulation and qualification determined by Oil Red O staining. (g) Intracellular triglyceride levels determined by enzymatic analysis (n = 3−4, *p < 0.05, #p < 0.01; control vs HCP/pDNA, HCP/MST1 vs HCP/pDNA, HCP/siMST1 vs HCP/pDNA; pDNA, nonfunctional plasmid; MST1, MST1 protein-coding plasmid; siMST1, functional plasmid-encoding siRNA of MST1).

estimated for comparisons. The transfection efficiency increased with the increase in N/P ratios and later, stayed constant or decreased while the N/P ratio continued to increase.

Plasmid-encoding green fluorescent protein (GFP) was delivered and observed in both cell lines (Figure 1e). The percentages of GFP-positive cells in the Hep@PGEA, CD-PGEA, and PEI groups in the HepG2 cell line were 31 ± 1, 13 ± 2, and 23 ± 2%, respectively, while they were 36 ± 2, 25 ± 2, and 18 ± 1%, respectively, in the AML-12 cell line. More positive cells were observed in the Hep@PGEA-treated group than in groups treated with CD-PGEA and PEI, which was per the luciferase expression results shown in Figure 1d.

https://doi.org/10.1021/acsami.2c05889
ACS Appl. Mater. Interfaces 2022, 14, 34328−34341

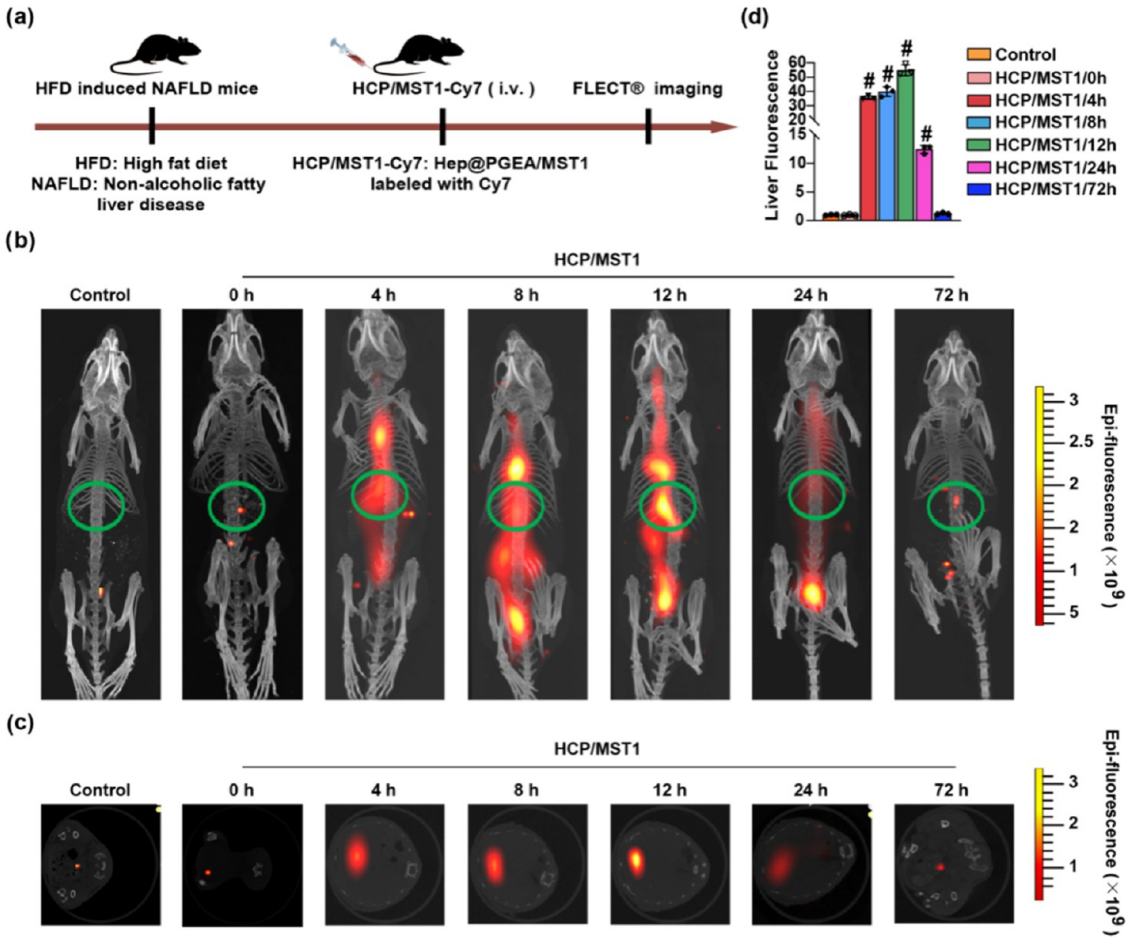

Figure 3. In vivo distribution of HCP/MST1 complexes in NAFLD mice. (a) Diagram of the injection models of HCP/MST1 complexes. (b) HCP/MST1 fluorescent enrichment levels at different times. (c, d) HCP/MST1 in mouse liver fluorescent enrichment levels at different times (n = 3, #p < 0.01; MST1, MST1 protein-coding plasmid).

The above experiments have proved that the unlockable Hep@PGEA vector performed better than CD-PGEA and PEI by delivering model plasmids. We further confirmed the efficiency of the Hep@PGEA vector in delivering different plasmids using cellular uptake assays (Figure S2). No significant difference in fluorescent signals was observed in AML-12 cells treated with HCP/pDNA complexes (condensing YOYO-1 labeled negative control plasmid pDNA), HCP/MST1 complexes (condensing YOYO-1 labeled MST1 plasmid), and HCP/siMST1 complexes (condensing YOYO-1 labeled siMST1 plasmid). The corresponding flow cytometry analysis confirmed the endocytosis results. The cellular uptake results indicated that the Hep@PGEA vector can also efficiently deliver MST1 and siMST1 plasmids.

To determine whether Hep@PGEA-delivered functional plasmids can efficiently regulated the expression of targeted MST1, we added well-mixed HCP/MST1 or HCP/siMST1 complexes (Hep@PGEA/siMST1 complexes, the Hep@PGEA vector condensed with plasmid-encoding siRNA of MST1) to the AML-12 cells in the presence or absence of 250 μM palmitic acid (PA), a commonly recognized NAFLD cell model.[14] As shown in Figure 1f–h, the mRNA and protein levels of MST1 in AML-12 cells were significantly inhibited by PA. Interestingly, the Hep@PGEA vector successfully delivered both MST1 plasmid and siMST1, as indicated by the significant increase in MST1 mRNA and protein expression in the HCP/MST1 group and the significant decrease in the HCP/siMST1 group owing to the intervention of PA.

2.3. Hep@PGEA-Based Delivery System Regulates Hepatocyte Lipid Stacking via the AMPK/SREBP-1c Signaling Axis. To reveal that MST1, an energy sensor, is required for hepatic lipid homeostasis, we retrieved the human SREBP-1c or FAS promoter and clarified the components that targeted the MST1 effect. In HepG2 cells, MST1 significantly suppressed the transcriptional activation of wild type (WT) SREBP-1c promoter (−257/+90) (Figure S3a). The disruption of the SRE base order in the same promoter enhanced basal gene transcription and prevented the changes induced by MST1 (Figure S3a). MST1 overexpression also suppressed FAS promoter (−166/0) transcriptional activity, an effect that was inhibited by the destruction of the SRE base in the FAS promoter (Figure S3b). Moreover, hepatic MST1 knockdown significantly increased the basal activity of SREBP-1c and FAS promoters (Figure S3c,d). Interestingly, dominant-negative MST1 (DN-MST1 or MST1 K59R) disrupts WT MST1's ability to increase endogenous SREBP-1c and FAS transcription and expression (Figure S3e,f). Furthermore, our CHIP assay results indicated that the combination of SREBP-1 to the SRE motif in the SREBP-1c and FAS promoters decreased upon MST1 overexpression but increased upon MST1 knockdown (Figure S3g,h). The above results show that

https://doi.org/10.1021/acsami.2c05889
ACS Appl. Mater. Interfaces 2022, 14, 34328−34341

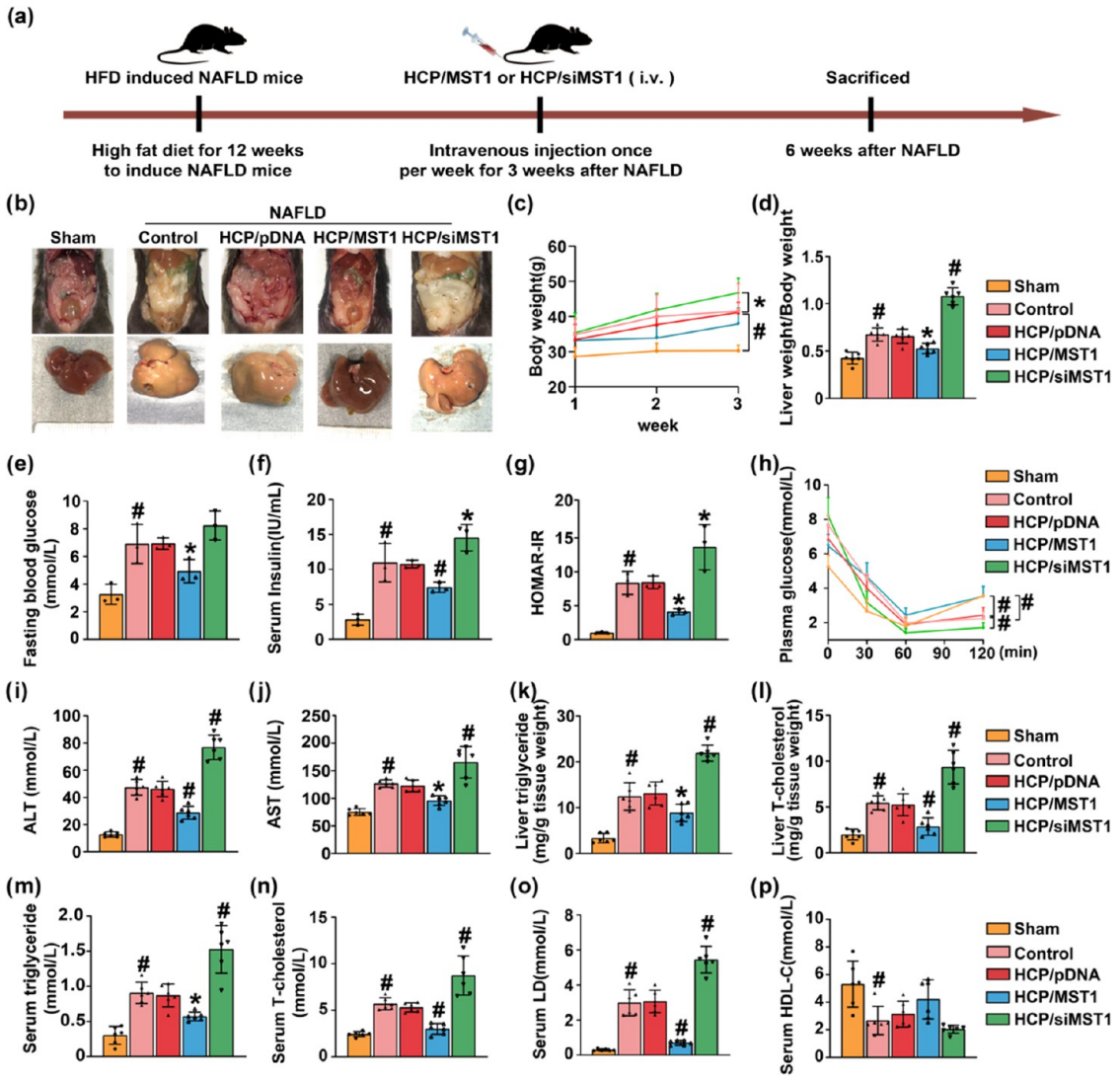

Figure 4. Reversible regulation of NAFLD with HCP/MST1 or HCP/siMST1 complexes. (a) Schematic diagram for injection models of HCP/MST1 or HCP/siMST1 or HCP/pDNA in NAFLD mice. C57BL/6 mice were fed a high-fat diet for 12 weeks before being injected with HCP/MST1 or HCP/siMST1 for 3 weeks. The tissues were harvested 6 weeks after NAFLD. (b) Phenotypic pattern of liver tissue captured by a digital camera. (c, d) Changes in body weight and liver weight/body weight in each group with various treatments. (e) Fasting blood glucose level. (f) Serum insulin levels. (g) Homeostasis model assessment-insulin resistance (HOMA-IR) level (h) ITT, insulin tolerance test. (i, j) Serum ALT and AST levels. (k–p) Lipid content in liver and serum (n = 3–6, *p < 0.05, #p < 0.01; control vs sham, HCP/MST1 vs HCP/pDNA, HCP/siMST1 vs HCP/pDNA. Sham: mice fed with a normal chow diet; pDNA, nonfunctional plasmid; MST1, MST1 protein-coding plasmid; siMST1, functional plasmid-encoding siRNA of MST1; ALT: alanine transaminase, AST: aspartate transaminase).

the SRE base order is responsible for the SREBP-1c and FAS transcription suppression of MST1.

We hypothesized that MST1 may suppress SREBP-1c activity through protein interactions and/or phosphorylation. When five overlapping Myc-tagged SREBP-1c regions (peptides F1-F5) were immunoprecipitated, HA-tagged MST1 precipitated with the following two peptides: F1 (1–231 aa) and F2 (223–445 aa), both of which contain the SREBP-1c nuclear form domain (Figure S4a). These results indicate that MST1 is not only combined with the SREBP-1c precursor, but also with the nuclear form of the protein. We therefore searched for consensus MST1 recognition sites within the human SREBP-1c sequence. Bioinformatics analysis intended to identify putative MST1 phosphorylation sites within the human SREBP-1c aa sequence identified serine 372 (Ser372), located in the N-terminal region of SREBP-1c F2 (Figure S4b). As shown in Figure S4c,d, the WT nuclear forms of SREBP-1c, including the phosphorylated S372D mutant, were directly and potently phosphorylated by MST1 in vitro and in vivo. The S372A mutation eliminated MST1-induced SREBP-1c phosphorylation. Importantly, MST1 phosphorylated SREBP-1c at Ser372 in both the cytoplasm and the nucleus, showing that the N-terminal area of MST1 is necessary for its protein kinase domain function (Figure S4d). Moreover, Ser372 phosphorylation was ablated by the MST1 K59R mutant plasmid in vitro and in vivo (Figure S4e,f). These results were confirmed by those of our immunoblotting and fluorescent protein analyses, indicating that MST1 specifically phosphorylates Ser372 (Figures S5–S7). These data confirm that MST1, as an upstream kinase, is of great significance in endogenous SREBP-1c phosphorylation.

Taken together, the above findings indicate that MST1 is sufficient to downregulate SREBP-1-dependent fat genetic

https://doi.org/10.1021/acsami.2c05889
ACS Appl. Mater. Interfaces 2022, 14, 34328–34341

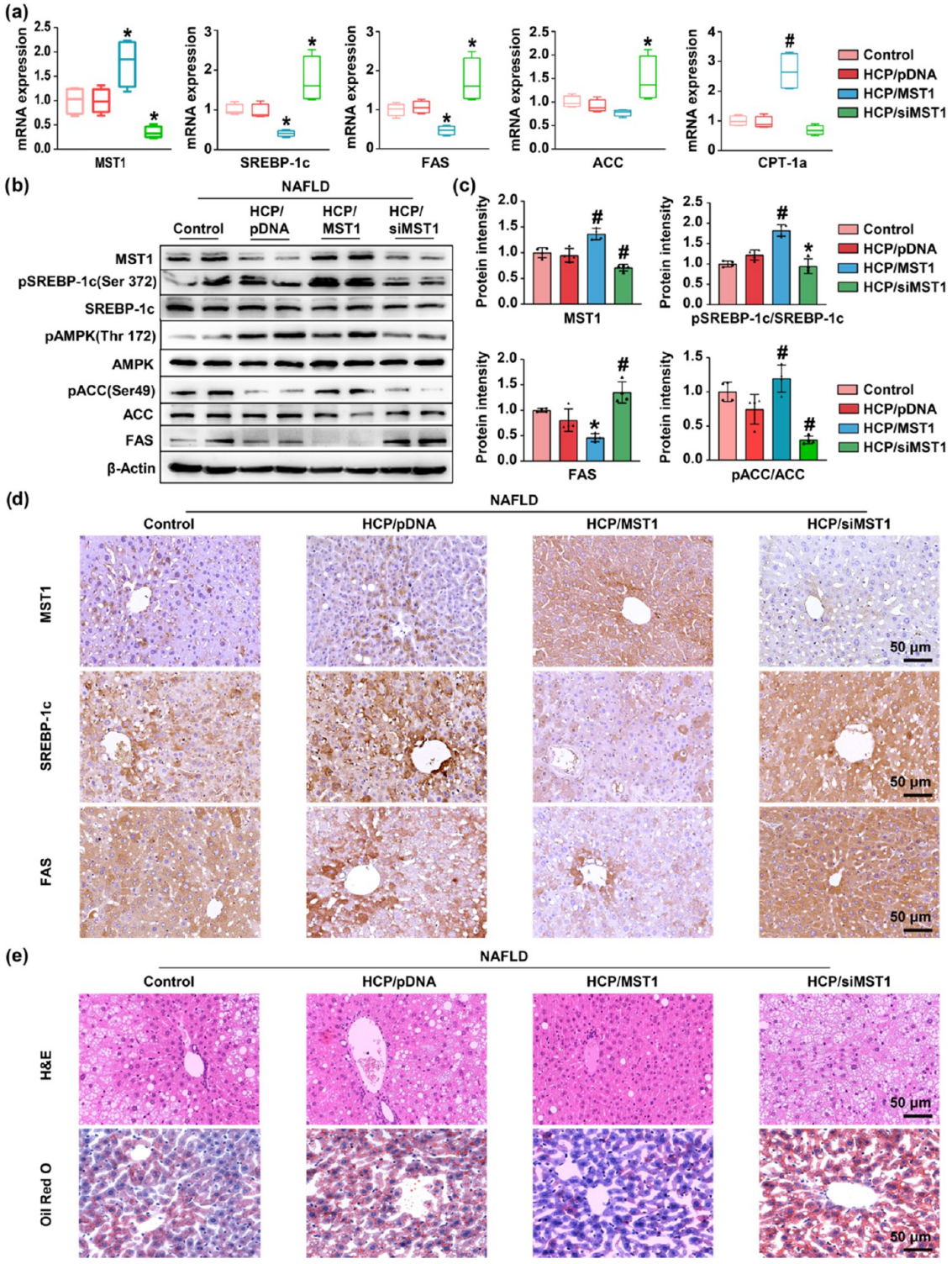

Figure 5. Hep@PGEA-based MST1 or siMST1 delivery system regulates NAFLD via the AMPK/SREBP-1c signaling axis. (a) mRNA levels of lipogenic genes in the liver. (b, c) Western blot (WB) analysis of MST1 and related protein expression levels in the liver. (d) Representative IHC images of lipogenic key factors in the liver. (e) H&E and Oil Red O staining of mouse liver ($n = 3–4$, $^*p < 0.05$, $\#p < 0.01$; HCP/MST1 vs HCP/pDNA, HCP/siMST1 vs HCP/pDNA; pDNA, nonfunctional plasmid; MST1, MST1 protein-coding plasmid; siMST1, functional plasmid-encoding siRNA of MST1).

transcription in liver cells to inhibit DNL, which is essential for NAFLD attenuation. Targeting MST1 may represent a feasible and effective strategy for combating NAFLD. We have demonstrated that Hep@PGEA successfully delivered the MST1 or siMST1 nucleic acid to regulate the MST1 level (Figure 1f–h). Then we verify the therapeutic capacity of Hep@PGEA-Based MST1 delivery systems in vitro. HCP/MST1 complexes inhibited SREBP-1c transcription by stimulating the phosphorylation of SREBP-1c phosphate, reducing the expression of FAS. The complexes also affected

https://doi.org/10.1021/acsami.2c05889
ACS Appl. Mater. Interfaces 2022, 14, 34328–34341

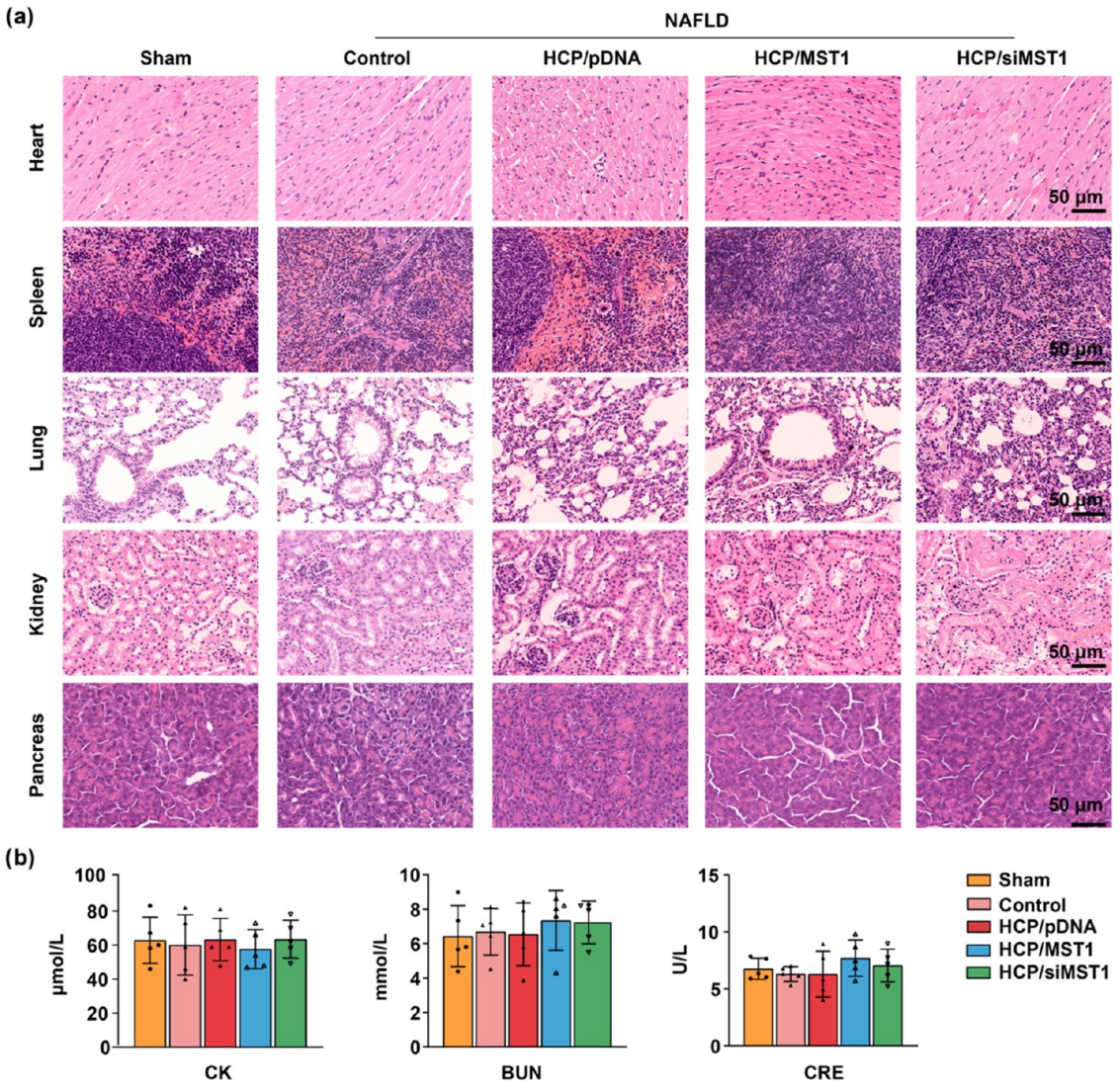

Figure 6. (a) Representative images of H&E staining of main organs. (b) Plasma biochemical tests of creatine kinase (CK), blood urea nitrogen (BUN), and creatinine (CRE).

the phosphorylation of AMPK and acetyl-coA carboxylase (ACC), leading to increased CPT-1a expression and fatty acid oxidation in hepatocytes (Figure 2a–c). Immunofluorescence analysis further confirmed the regulating abilities of Hep@PGEA/MST1 and Hep@PGEA/siMST1 complexes (Figure 2d).

We next examined the lipid content in hepatocytes to investigate the therapeutic ability of the Hep@PGEA-based MST1 delivery system. Oil Red O staining results indicated that HCP/MST1 complexes could significantly reduce lipid accumulation in AML-12 cells exposed to PA conditions, while the intracellular triglyceride (TG) level was also reduced (Figure 2e–g). These results proved that Hep@PGEA can efficiently deliver MST1 or siMST1 into hepatocytes and successfully regulate lipid accumulation in steatosis hepatocytes, which indicates its considerable potential in restoring hepatic steatosis for NAFLD therapy.

2.4. Hep@PGEA Successfully Delivered Functional Nucleic Acids to the NAFLD Mouse Liver. A group of mice was set up an NAFLD model under the feeding conditions of high-fat diet (HFD). The HCP/MST1 group was administered HCP/MST1 complexes, and the control group was administered PBS (Figure 3a). The liver enrichment and changes following the HCP/MST1 complex administration over time were photographed (Figure 3b,c). The fluorescent signals in the kidney and other organs in NAFLD mice were weak. The fluorescence of the NAFLD mouse liver indicated considerable accumulation of HCP/MST1 complexes, which first increased and then decreased with time (Figure 3b–d).

2.5. Hep@PGEA Vector-Mediated NAFLD Gene Therapy In Vivo. The Hep@PGEA vector has been proven to efficiently deliver both MST1 and siMST1 for the intervention of NAFLD in vitro, and the abundant accumulation of the Hep@PGEA-based delivery system in the liver further confirmed its potential for use in NAFLD therapy (Figure 4). NAFLD mice were divided into different groups and treated with PBS as the control group, Hep@PGEA/pDNA complexes (pDNA, nonfunctional plasmid) as the HCP/pDNA group, Hep@PGEA/MST1 complexes (MST1, MST1 protein-coding plasmid) as the HCP/MST1 group, and Hep@PGEA/siMST1 complexes (siMST1, function plasmid-encoding siRNA of MST) as the HCP/siMST1 group. The mice fed with a normal diet were retained as the sham group (Figure 4a).

https://doi.org/10.1021/acsami.2c05889
ACS Appl. Mater. Interfaces 2022, 14, 34328–34341

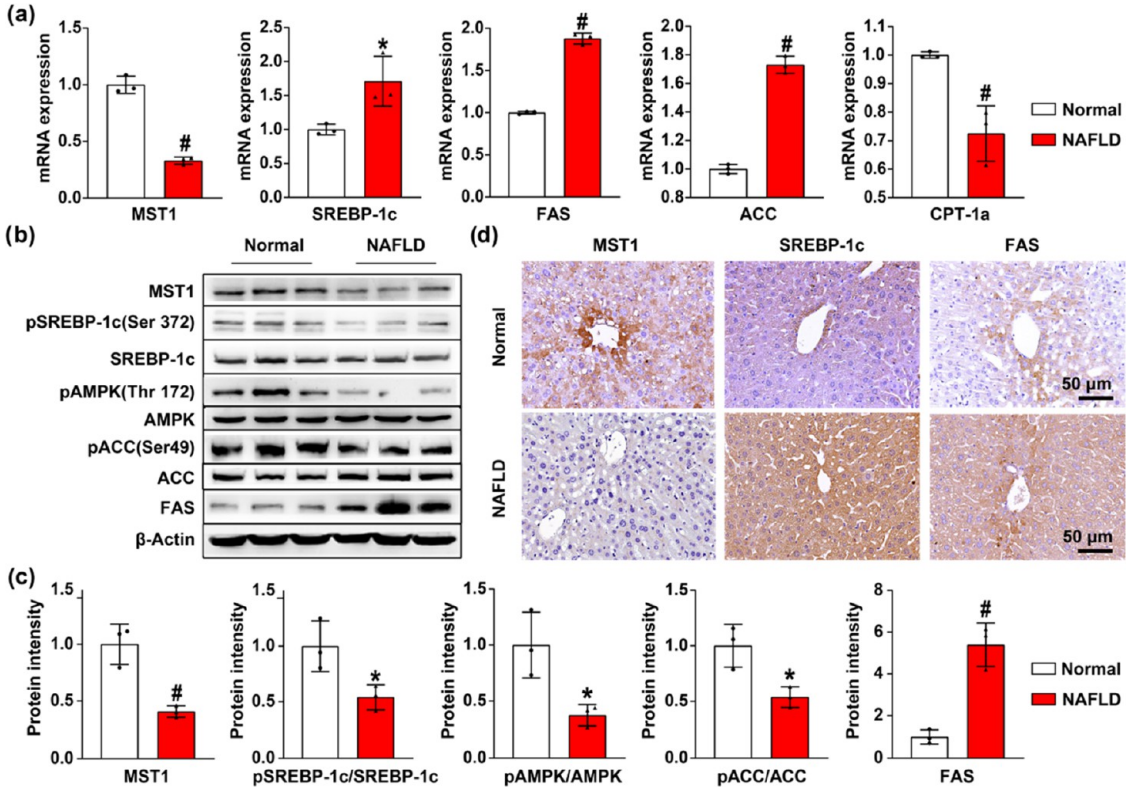

Figure 7. Hepatic MST1 expression and lipogenic factors in patients with NAFLD. (a) mRNA levels of MST1 and lipogenic genes. (b−d) Protein levels of MST1 and lipogenic proteins (n = 3, *p < 0.05, #p < 0.01; normal vs NAFLD).

As shown by the liver morphology studies, compared to sham mice, the livers of NAFLD mice in the control group were larger and the surface was covered with fine yellow lipid particles. The accumulation of lipid droplets on the liver surface in the HCP/siMST1 group was more serious, while fewer lipid droplets were observed on the liver surface in the HCP/MST1 group (Figure 4b). The changes in body weight and liver weight/body weight of mice were similar between groups (Figure 4c,d).

Insulin resistance (IR) is the classic hypothesis of NAFLD pathogenesis, which causes lipid accumulation in liver cells and leads to increased sensitivity of the liver to internal factors.[11] Therefore, inhibiting liver IR is a powerful initiative for treating NAFLD. The FBG and insulin levels in the control group were remarkably higher than those in the sham group and were further increased in the HCP/siMST1 group but significantly decreased in the HCP/MST1 group (Figure 4e,f). The homeostasis model assessment-insulin resistance (HOMA-IR) value in the HCP/MST1 group of the NAFLD mice decreased significantly (Figure 4g). The analysis of the oral glucose tolerance test (OGTT) (Figure S8) and insulin tolerance test (ITT) (Figure 4h) implied that the glucose clearance rate of mice in the control group was highly lower than that in the sham group.

We also tested the serum alanine transaminase (ALT) and aspartate transaminase (AST) levels to evaluate liver damage. As shown in Figure 4i,j, ALT and AST levels in the control group were higher than those in the sham group. The ALT and AST levels increased significantly in the HCP/siMST1 group but decreased significantly in the HCP/MST1 group. Lipid content in the liver and the serum was also evaluated (Figure 4k−p). Compared with the sham group, the mice with NAFLD in the control group exhibited more hepatic lipid deposits, which were mainly reflected in high levels of triglyceride (TG), total cholesterol (TC), and low-density lipoproteins (LDL). The Hep@PGEA/MST1 delivery system significantly reduced the TG, TC, and LDL levels in NAFLD mice. These results not only certificated the Hep@PGEA vector capable of providing functional nucleic acids for NAFLD regulation but also proved that Hep@PGEA/MST1 complexes can improve IR to reduce the liver damage caused by hepatic steatosis, which offers a promising option for NAFLD treatment.

2.6. Hep@PGEA-Based MST1 or siMST1 Delivery System Regulates NAFLD via the AMPK/SREBP-1c Signaling Axis. Based on the findings regarding the regulatory ability of the Hep@PGEA-based delivery system in NAFLD therapy, we next analyzed the signaling axis to confirm its efficiency (Figure 5). Compared with the control group, the phosphorylation level of SREBP-1c, AMPK, and ACC was inhibited, and the expression of FAS was increased considerably when the MST1 expression was downregulated with Hep@PGEA/siMST1 complexes in the HCP/siMST1 group (Figure 5a−c). MST1 expression was upregulated in the liver of the NAFLD mice administered with Hep@PGEA/MST1 complexes, and this benefited the phosphorylation of SREBP-1c at Ser372 to suppress the SREBP-1c cleavage and nuclear translocation, promoted the phosphorylation of AMPK, and reduced the expression of FAS in hepatocytes (Figure 5a−c). Immunohistochemistry analysis further confirmed the changes in the MST1, SREBP-1c, and FAS protein levels (Figure 5d). H&E and Oil Red O staining results confirmed that Hep@PGEA/MST1 complex-treated NAFLD mice (HCP/MST1) exhibited clear hepatic cell cords,

https://doi.org/10.1021/acsami.2c05889
ACS Appl. Mater. Interfaces 2022, 14, 34328−34341

complete liver lobular structures, less liver injury, and fewer small bladder lipid droplets (Figure 5e). These results indicate that Hep@PGEA vectors successfully deliver MST1 or siMST1 for NAFLD intervention through the AMPK/SREBP-1c signaling axis. The HEP@PGEA-based MST1 delivery system can reduce liver lipid biosynthesis and regulate hepatic lipid metabolism through promoting SREBP-1c and AMPK phosphorylation, thereby providing a hopeful choice for NAFLD treatment.

2.7. Biosafety of the Hep@PGEA-Mediated Gene Delivery Stragety. One of the key factors that limit the application of polycation vectors is their toxicity in vivo. We analyzed the toxicity caused by various treatments to evaluate the potential of the Hep@PGEA vector in NAFLD therapy. The body weight of each group was measured for 3 weeks after injection. The data shown in Figure 6b indicates no significant weight loss. Organs, including the heart, spleen, lung, kidney, and pancreas, from different groups, were also sectioned and stained with H&E. No abnormalities of the histological structure were observed in the organs (Figure 6a). Biochemistry tests including liver function (ALT and AST levels), cardiac toxicity (CK level), and renal function (BUN and CRE levels) tests were also performed. In HFD-induced NAFLD mice, ALT and AST levels were elevated, indicating that HFD accelerates liver IR. Moreover, the administration of Hep@PGEA/MST1 complexes significantly weakened the liver IR caused by NAFLD and restored liver function (Figure 4i,j). No statistically significant difference in CK, BUN, and CRE levels was observed in any of the groups (Figure 6b). These results suggest that systemic administration of Hep@PGEA/MST1 complexes efficiently inhibits HFD-induced NAFLD development without causing significant toxicity.

2.8. Analysis of NAFLD Patient Samples. To investigate the possibility of clinical application of gene therapy targeting MST1 for NAFLD patients, we then analyzed liver tissues of healthy people and NAFLD patients. The hepatic steatosis was confirmed by H&E staining (Figure S9). The mRNA levels of MST1 and lipogenic genes in the patients with NAFLD were significantly changed compared to those of healthy people (normal group) (Figure 7a). The expression of MST1 protein in the cytoplasm and nucleus of NAFLD patients was reduced (Figure 7b–d). The phosphorylation levels of SREBP-1c, AMPK, and ACC were decreased, while the level of FAS was markedly elevated in patients with NAFLD (Figure 7b–d). These findings are consistent with those of NAFLD mice models. Taken together, our results demonstrated that Hep@PGEA-based delivery of MST1 in vivo is a promising therapeutic option for patients with NAFLD.

3. DISCUSSION

This study reveals the therapeutic benefits of the Hep@PGEA-based MST1 (HCP/MST1) gene delivery system on non-alcoholic fatty liver disease (NAFLD) by the AMPK/SREBP-1c pathway. We found that the HCP/MST1 complexes significantly improved liver insulin resistance (IR), repressed hepatic lipogenesis, and promoted liver fat oxidation, while Hep@PGEA-based siMST1 (HCP/siMST1) gene delivery exacerbated the NAFLD process.

The most prominent metabolic characteristic of NAFLD is the DNL or IR effect.[25−27] Another typical metabolic change characteristic of fatty hepatocytes is an abnormal increase of transcription factors, such as SREBP, liver X receptor (LXR)/retinoid X receptor (RXR), and peroxisome proliferator-activated receptor γ (PPARγ)/PPARγ coactivator-1β (PGC-1β).[28−31] As fatty acids are essential constituents of biological membrane lipids, NAFLD progression occurs only when there is excessive intracellular accumulation. DNL is triggered by upregulated transcription factor SREBP-1c during NAFLD progression.[28,32]

Studies have reported that MST1 exerts a protective effect on NAFLD through Sirt1 ubiquitination.[19] Our previous studies also prove that the excessive expression of MST1 in the liver caused changes in the AMPK/SREBP-1c signaling cascade, which subsequently affects CPT-1α and FAS levels and reduces the accumulation of liver lipids.[15] In summary, we propose that targeting MST1 in the AMPK/SREBP-1c signaling axis may represent a practicable and effective policy for combating NAFLD.

Due to various obstacles in vivo, vectors were needed for delivering and protecting functional nucleic acids prior to releasing them. Polycation-based vectors have attracted widespread attention, especially the ethanolamine (EA)-modified poly(glycidyl methacrylate) (PGEA) vectors with abundant hydroxyl groups for extended circulation.[22] The recently developed Hep@PGEA vector with self-accelerating release for condensed nucleic acids in response to reductants in cells (such as GSH) showed impressive performance in the treatment of both cardiovascular disease and cancer as a gene vector for either RNA or DNA.[23,24] In this study, we focused on whether Hep@PGEA vectors efficiently delivered the MST1 or siMST1 functional for NAFLD regulation, and how HCP/MST1 or HCP/siMST1 complexes regulated liver function in NAFLD mouse models by modulating the AMPK/SREBP-1c signaling axis (Scheme 1).

We first proved that the Hep@PGEA vector successfully delivered and released MST1 and siMST1 for the intervention of NAFLD via the AMPK/SREBP-1c signaling axis in vitro (Figures 1 and 2). Then, the HCP/MST1 complexes were administered to HFD-induced NAFLD mice models as the representative and corresponding accumulations of HCP/MST1 complexes in the liver were recorded. Significant and sustained signals were observed in the liver (Figure 3). The significant accumulation confirmed the high enrichment as well as the long retention time of HCP/MST1 complexes in mouse liver, which proved the potential of the Hep@PGEA vector in delivering MST1 for NAFLD therapy. The plentiful hydroxyl groups in the Hep@PGEA vector can form a hydrating layer that surrounds the HCP/MST1 complexes, which hinder protein absorption on the complexes and protect them from clearance by mononuclear phagocytes. Thus, the HCP/MST1 complexes showed extended circulation and retention times in vivo,[22] which will further benefit Hep@PGEA-based gene therapy for NAFLD in vivo.

Hep@PGEA/MST1 or Hep@PGEA/siMST1 complexes were administered to HFD-induced NAFLD mice through tail venous retransmission for 3 weeks. The organs were collected and analyzed after various treatments (Figures 4–6). We found that the accumulation of lipids on the liver is more serious in the HCP/siMST1 group, while the HCP/MST1 group effectively alleviates the damage (Figure 4). We also proved that the HCP/MST1 complex treatment suppresses the transcription of SREBP-1c to suppress the expression of FAS, stimulates AMPK phosphorylation to increase CPT-1a expression, and finally, reduces the synthesis of liver fat and accelerates the oxidation of liver fatty acids (Figure 5). These results can be attributed to the high level of accumulation and

https://doi.org/10.1021/acsami.2c05889
ACS Appl. Mater. Interfaces 2022, 14, 34328−34341

long retention time of the Hep@PGEA-based delivery system. High redox components (such as GSH) also contribute to the release of condensed nucleic acids (Figure 1a,b), which further improve the efficiency of Hep@PGEA vectors and provide impressive intervention results without inducing significant abnormal changes in the organs (Figure 6).

To confirm the clinical relevance of this study, we analyzed a set of NAFLD patient samples (Figure 7). RT-PCR, WB, and immunohistochemical analyses confirmed the influence of the AMPK/SREBP-1c signaling axis on the progression of NAFLD in humans, which is consistent with our experiment results. The value of MST1 in the development of liver fat degeneration in NAFLD patients was also confirmed, suggesting that the Hep@PGEA-based MST1 gene delivery might be a potential therapeutic option to reduce liver lipid accumulation, ameliorate liver injury, and treat clinical NAFLD.

4. CONCLUSIONS

In this study, we proposed and proved the application of the Hep@PGEA-based MST1 gene delivery system (HCP/MST1) for NAFLD gene therapy. The Hep@PGEA vector can efficiently transport condensed functional nucleic acids into the NAFLD mouse liver, following which the high redox levels, such as GSH, in the liver, further accelerate the release of condensed nucleic acids due to the redox-triggered unlockable structure of the Hep@PGEA vector. We also demonstrated that the HCP/MST1 complexes significantly improved liver IR sensitivity and reduced liver damage and liver lipid accumulation by adjusting the AMPK/SREBP-1c signaling pathway, providing a potential strategy for NAFLD therapy without any significant toxicity. The analysis of NAFLD patient samples further proved the important value of MST1 in the progress of liver fat degeneration in NAFLD patients. The study indicates that MST1-based gene intervention is of great potential for clinical NAFLD therapy and that the Hep@PGEA vector provides a promising option for NAFLD gene therapy, thus reducing the NAFLD burden.

5. EXPERIMENTAL SECTION

5.1. Reagents and Antibodies. Branched polyethylenimine (PEI, M_W ~25000 Da), tetrabutylammonium chloride (TBA, 98%), α-lipoic acid (LA, 99%), 4-(dimethylamino)-pyridine (DMAP, 98%), streptomycin, penicillin, dicyclohexylcarbodiimide (DCC, 98%), sodium borohydride (NaBH4, 98%), and palmitic acid were obtained from Sigma-Aldrich Chemical Co. Methylthiazolyldiphenyl-tetrazolium bromide (MTT, 98%) was purchased from Energy & Chemical Co., Ltd. Renilla luciferase assay kits and dual-luciferase reporter assay kits were purchased from Promega. The triglyceride and cholesterol assay kits were gained from Applygen Technologies Inc., Beijing, China. TRIzol and lipofectamine 3000 transfection reagent were purchased from Invitrogen.

Anti-SREBP-1c antibody (#14088-1-AP) was purchased from Proteintech. Anti-MST1 (#3682), anti-AMPK (#5831), anti-phospho-AMPK (#2535), anti-phospho-SREBP-1c (#9874), anti-Acetyl-CoA carboxylase (ACC) (#3662), and anti-phospho-ACC (#3661) antibodies were obtained from Cell Signaling Technology. Anti-FAS antibody (#Ab22759) was purchased from Abcam (Cambridge, UK).

5.2. Construction and Characterization of MST1 Overexpression and RNA Interference Nucleic Acids. Overexpression plasmid and RNA interference nucleic acids were constructed to upregulate or downregulate the level of MST1. Primers were designed to amplify mouse full-length MST1 cDNA and infixed into the lentivirus overexpression vector p_CDNA3 between the Nhe I and Sal I sites. Meanwhile, the shRNA sequence was synthesized and infixed into the pGreenPuro vector to obtain siMST1 (encoding MST1 siRNA) or siCtrl (encoding negative control siRNA). The primers used in this process are listed in Table S1. Empty or MST1 plasmids, siCtrl, or siMST1 was transfected into mouse normal liver cells (AML-12 cells) separately with transfection reagent under the guidance of the instructions.

5.3. Preparation of Charge-Reversal Heparin-Based Gene Vector in Response to Reductants. As reported earlier, negatively charged heparin locked by disulfides as a core in the Hep@PGEA vector endows the vector with the charge-reversal ability required for the self-accelerating release of condensed nucleic acids.[24] The Hep@PGEA vector was prepared as has been described previously.[24] The heparin nanoparticles obtained were called HepNPs. Cationic PGEA was then prepared via a ring-opening reaction of the β-CD-cored poly(glycidyl methacrylate) with EA (CD-PGEA). The core−shell nanocomplex Hep@PGEA was prepared at a weight ratio of 5 (WCD-PGEA/WHepNP) and used for the following investigations.

5.4. Biophysical Characterization of the Hep@PGEA Vector. Plasmid-encoding MST1 protein was used for biophysical characterization of the Hep@PGEA vector as a representative. To determine the condense and release ability of the Hep@PGEA vector for MST1, a ζ-sizer Nano ZS was used to confirm the particle size and ζ-potential of Hep@PGEA/MST1 at different Hep@PGEA to MST1 ratios.[24] The Hep@PGEA to MST1 ratio was expressed as the ratio of nitrogen (N) in CD-PGEA to phosphorus (P) in MST1 plasmid (or termed as the N/P ratio).

5.5. Cytotoxicity Assays. Immortalized AML-12 cells were cultured in a DMEM/F12 medium (Hyclone) containing 10% FBS (Gibco), 100 U/mL penicillin, and 100 μg/mL streptomycin (PS) in an incubator at 37 °C and 5% CO_2 atmosphere. Additionally, HepG2 cells were cultured in DMEM containing FBS and PS under the same conditions.

The viability of the HepG2 and AML-12 cell lines was evaluated to assess the potential of Hep@PGEA as a delivery vehicle for NAFLD. Briefly, the cells were inoculated in 96-well plates and cultivated for 24 h. Two concentrations of the polycation/pDNA complexes at different N/P ratios were prepared and added to the wells. Different concentrations of complexes were obtained by adjusting the administered quantity of pDNA (0.33 μg of pDNA/well for 1× and 1 μg of pDNA/well for 3×).[24]

5.6. Transfection Assays. For transfection assays, HepG2 or AML-12 cells were seeded into 24-well plates at a density of 5×10^4 cells per well and cultured for 24 h. Two concentrations of the polycation/pDNA complexes at different N/P ratios were added to the wells and incubated for 18 h, and the concentration was determined based on the dose of pDNA (1× contained 1 μg of pDNA/well and 3× contained 3 μg of pDNA/well). Corresponding transfection efficacy was measured using a Renilla luciferase assay kit.[22]

To confirm the transfection efficiency of the Hep@PGEA vector, we examined the enhanced green fluorescent protein (EGFP) expression in the HepG2 or AML-12 cell lines induced by Hep@PGEA, CD-PGEA, and PEI at the N/P ratios of 15, 15, and 10 (containing 3 μg of pEGFP/well). EGFP signals were observed and imaged using a fluorescent microscope. The above experiments demonstrate the advantages of the Hep@PGEA vector in delivering the genetic material to liver-related cells.

5.7. Functional Nucleic Acids Delivered with the Hep@PGEA Vector In Vitro. AML-12 cells were then seeded in a six-well plate and cultured for 24 h at a density of 4×10^5. They were then serum-starved for 2 h and treated for 18 h in a serum-free medium of phosphate-buffered saline (control group), Hep@PGEA/pDNA complexes (N/P = 15, containing 3 μg of pDNA, HCP/pDNA group), Hep@PGEA/MST1 complexes (N/P = 15, containing 3 μg of MST1, HCP/MST1 group), and Hep@PGEA/siMST1 complexes (N/P=15, containing 3 μg of siMST1, HCP/siMST1 group).

The expression of MST1 was evaluated to confirm the efficiency of Hep@PGEA-delivered MST1 or siMST1 using RT-PCR assay and WB. Moreover, immunofluorescence was used to detect the MST1 and lipogenic markers. Briefly, after the treated cells were fixed with

https://doi.org/10.1021/acsami.2c05889
ACS Appl. Mater. Interfaces 2022, 14, 34328−34341

4% paraformaldehyde, cell membrane permeability treatment was carried out successively; 5% bovine serum albumin was blocked; cells were incubated with anti-MST1, anti-FAS, or anti-SREBP-1c antibodies overnight and then with goat Anti-Rabbit IgG H&L (Alexa Fluor 568) for 1 h; nuclear staining was performed; and then, an electron fluorescence microscope was used to collect and analyze the images.

Oil Red O staining was performed and intercellular triglyceride content was detected according to the manufacturer's instructions to evaluate the accumulation of liver cell lipids to confirm the efficiency of the Hep@PGEA vector in delivering MST1 or siMST1 to upregulate or downregulate the MST1 protein level in NAFLD therapy.

5.8. Accumulation of Hep@PGEA-Mediated MST1 Gene Delivery in NAFLD Mice. All animal experiment actions involved in the study were authorized by the Animal Care and Use Committee of the Institute of experimental animals, Chinese Academy of Medical Sciences and Beijing Union Medical College (yzw19006).

NAFLD mice were used to evaluate the accumulation of Hep@PGEA-mediated MST1 gene delivery in the liver. The HCP/MST1 group mice were administered 150 μL solution of Hep@PGEA/MST1 complexes (N/P = 15, containing 30 μg of MST1 plasmid) via tail vein injection, while the control group comprised of mice administered with an equal volume of PBS. The Hep@PGEA vector was labeled using a Cy7 fluorescent molecule at a weight ratio of 1000:1 (WHep@PGEA:WCy7) before condensation of MST1 plasmid. The accumulation of Hep@PGEA/MST1 complexes in mice was detected and photographed with a Trifoil InSyTe FLECT imager (β version, TriFoil Imaging), following previously described.[15]

5.9. Hep@PGEA Vector-Mediated NAFLD Gene Therapy In Vivo. Mice that were fed a normal chow diet were used as sham. The NAFLD mice were given a high-fat diet (HFD) and were divided into four groups of 10 mice each. The control group was administered 150 μL of PBS, the HCP/pDNA group was administered 150 μL of Hep@PGEA/pDNA complexes (N/P = 15, containing 30 μg of pDNA), the HCP/MST1 group was administered 150 μL of Hep@PGEA/MST1 complexes (N/P = 15, containing 30 μg of MST1 plasmid), and the HCP/siMST1 group was administered 150 μL of Hep@PGEA/siMST1 complexes (N/P = 15, containing 30 μg of siMST1 plasmid). All of the administrations were performed via the tail vein, once a week, for three weeks.

The body weights of the mice were monitored each week, and the fasting blood glucose (FBG) level and the glucose tolerance and insulin tolerance levels of the mice were monitored at the end of the experiment period as described previously..[14,15] The biochemical indexes of mouse plasma were detected by a biochemical analyzer. The mice were subsequently sacrificed and their organs were collected. Several sections of the livers were stored at −80 °C for RT-PCR and WB analysis, while the rest, along with the other organs were fixed and embedded in paraffin for pathological analysis, including H&E and immunohistochemical staining. According to the anatomical images of mouse liver, hematoxylin−eosin (H&E) staining and oil red O staining, observing the pathological changes and lipid deposition of mouse liver in each group, were observed. Immunohistochemical staining was performed as described previously[15] to detect the protein expression levels of MST1, SREBP-1c, and FAS in mouse liver.

5.10. MST1 Expression in NAFLD Patient Liver Samples. Human liver specimens were collected from 11 patients at the Ningxia Medical University Second Affiliated Hospital (Yinchuan, China). Experiments involving human liver specimens were performed per the directions of the Ethical Committee on Human Research of Ningxia Medical University and the other participating hospitals, and the patients provided written informed consent for the collection and use of their samples before participating in the study (approval number: 2019-228). The steatosis indices of these liver specimens were accessed by H&E staining. Based on the size and number of lipid droplets present in the liver specimens, we divided them into normal (n = 6) and NAFLD groups (n = 5). RT-PCR, WB, and immunohistochemistry analyses were performed to detect the MST1 expression and relative protein levels involved in the AMPK/SREBP-1c signaling axis.

5.11. Statistical Analysis. The data were statistically analyzed in GraphPad Prism 8 software and displayed as mean ± SD. T-test was used for comparison between the two groups, and one-way ANOVA was used for comparison between multiple groups, with a statistical difference of $p < 0.05$.

■ ASSOCIATED CONTENT

Supporting Information

The Supporting Information is available free of charge at https://pubs.acs.org/doi/10.1021/acsami.2c05889.

Cytotoxicity of polycation-based vectors in HepG2 and AML-12 cell lines at a high concentration; cellular uptake assay; MST1 represses the transcriptional activity of SREBP-1c and its lipogenic target genes; MST1 interacts with SREBP-1c and directly phosphorylates Ser372; motif scan graphic indicating that Ser372 of human SREBP-1 was phosphorylated by MST1 kinase; immunoblot analysis of p-SREBP-1c (Ser372) expression in NAFLD patients; MST1 induces SREBP-1c nuclear translocation; blood glucose levels in mice with various treatments, and hepatic steatosis determined by H&E in people with or without NAFLD (PDF)

■ AUTHOR INFORMATION

Corresponding Authors

Zhiwei Yang − *Beijing Engineering Research Center for Experimental Animal Models of Human Critical Diseases, Institute of Laboratory Animal Science, Chinese Academy of Medical Sciences (CAMS) & Comparative Medicine Centre, Peking Union Medical College (PUMC), Beijing 100021, China*; orcid.org/0000-0003-3006-2512; Email: yangzhiwei@cnilas.pumc.edu.cn

Fu-Jian Xu − *Key Lab of Biomedical Materials of Natural Macromolecules (Ministry of Education), Beijing Laboratory of Biomedical Materials, Beijing University of Chemical Technology, Beijing 100029, China*; orcid.org/0000-0002-1838-8811; Email: xufj@mail.buct.edu.cn

Yi Yang − *School of Basic Medical Sciences, Ningxia Medical University, Yinchuan 750004, China*; Email: yangyi0908666@163.com

Authors

Yuhan Li − *School of Basic Medical Sciences, Ningxia Medical University, Yinchuan 750004, China; Beijing Engineering Research Center for Experimental Animal Models of Human Critical Diseases, Institute of Laboratory Animal Science, Chinese Academy of Medical Sciences (CAMS) & Comparative Medicine Centre, Peking Union Medical College (PUMC), Beijing 100021, China*

Jing-Jun Nie − *Key Lab of Biomedical Materials of Natural Macromolecules (Ministry of Education), Beijing Laboratory of Biomedical Materials, Beijing University of Chemical Technology, Beijing 100029, China; Laboratory of Bone Tissue Engineering, Beijing Laboratory of Biomedical Materials, Beijing Research Institute of Traumatology and Orthopaedics, Beijing Jishuitan Hospital, Beijing 100035, China*

Yuhui Yang − *Capital Medical University, Beijing 100035, China*

Jianning Li − *School of Basic Medical Sciences, Ningxia Medical University, Yinchuan 750004, China*

Jiarui Li − *School of Basic Medical Sciences, Ningxia Medical University, Yinchuan 750004, China*
Xianxian Wu − *Beijing Engineering Research Center for Experimental Animal Models of Human Critical Diseases, Institute of Laboratory Animal Science, Chinese Academy of Medical Sciences (CAMS) & Comparative Medicine Centre, Peking Union Medical College (PUMC), Beijing 100021, China*
Xing Liu − *Beijing Engineering Research Center for Experimental Animal Models of Human Critical Diseases, Institute of Laboratory Animal Science, Chinese Academy of Medical Sciences (CAMS) & Comparative Medicine Centre, Peking Union Medical College (PUMC), Beijing 100021, China*
Da-Fu Chen − *Laboratory of Bone Tissue Engineering, Beijing Laboratory of Biomedical Materials, Beijing Research Institute of Traumatology and Orthopaedics, Beijing Jishuitan Hospital, Beijing 100035, China*

Complete contact information is available at: https://pubs.acs.org/10.1021/acsami.2c05889

Author Contributions

#Y.L., J.-J.N., and Y.Y. contributed equally to this work.

Author Contributions

Y.L., J.-J.N. and Y.Y. contributed equally to this work. J.L., J.L., X.W., and X.L. assisted in cell and animal experiments. All authors approved the final version of the manuscript.

Notes

The authors declare no competing financial interest.

■ ACKNOWLEDGMENTS

This work was supported in part by the National Natural Science Foundation of China (82160171, 81670798, 81970358, 51903013, and 51733001), Beijing Outstanding Young Scientist Program (BJJWZYJH01201910010024), Beijing Hospitals Authority Youth Programme (QML20210402), Beijing Jishuitan Hospital Nova Program (XKXX-202114), and Chinese Academy of Medical Sciences Innovation Fund for Medical Sciences (CAMS, 2021-I2M-1-072).

■ REFERENCES

(1) Chalasani, N.; Younossi, Z.; Lavine, J. E.; Charlton, M.; Cusi, K.; Rinella, M.; Harrison, S. A.; Brunt, E. M.; Sanyal, A. J. The Diagnosis and Management of Nonalcoholic Fatty Liver Disease: Practice Guidance from the American Association for the Study of Liver Diseases. *Hepatology* **2018**, *67*, 328−357.
(2) Younossi, Z. M.; Koenig, A. B.; Abdelatif, D.; Fazel, Y.; Henry, L.; Wymer, M. Global Epidemiology of Nonalcoholic Fatty Liver Disease-Meta-analytic Assessment of Prevalence, Incidence, and Outcomes. *Hepatology* **2016**, *64*, 73−84.
(3) Friedman, S. L.; Neuschwander-Tetri, B. A.; Rinella, M.; Sanyal, A. J. Mechanisms of NAFLD Development and Therapeutic Strategies. *Nat. Med.* **2018**, *24*, 908−922.
(4) Esler, W. P.; Bence, K. K. Metabolic Targets in Nonalcoholic Fatty Liver Disease. *Cell. Mol. Gastroenterol. Hepatol.* **2019**, *8*, 247−267.
(5) Cotter, T. G.; Rinella, M. Nonalcoholic Fatty Liver Disease 2020: The State of the Disease. *Gastroenterology* **2020**, *158*, 1851−1864.
(6) Younossi, Z. M.; Blissett, D.; Blissett, R.; Henry, L.; Stepanova, M.; Younossi, Y.; Racila, A.; Hunt, S.; Beckerman, R. The Economic and Clinical Burden of Nonalcoholic Fatty liver Disease in the United States and Europe. *Hepatology* **2016**, *64*, 1577−1586.
(7) Diehl, A. M.; Day, C. Cause, Pathogenesis, and Treatment of Nonalcoholic Steatohepatitis. *N. Engl. J. Med.* **2017**, *377*, 2063−2072.
(8) Zhang, W.; Lin, H.; Cheng, W.; Huang, Z.; Zhang, W. Protective Effect and Mechanism of Plant-Based Monoterpenoids in Non-alcoholic Fatty Liver Diseases. *J. Agric. Food. Chem.* **2022**, *70*, 4839−4859.
(9) Dessein, A. Clinical Utility of Polygenic Risk Scores for Predicting NAFLD Disorders. *J. Hepatol.* **2021**, *74*, 769−770.
(10) Caussy, C.; Soni, M.; Cui, J.; Bettencourt, R.; Schork, N.; Chen, C. H.; Ikhwan, M. A.; Bassirian, S.; Cepin, S.; Gonzalez, M. P.; Mendler, M.; Kono, Y.; Vodkin, I.; Mekeel, K.; Haldorson, J.; Hemming, A.; Andrews, B.; Salotti, J.; Richards, L.; Brenner, D. A.; Sirlin, C. B.; Loomba, R. Nonalcoholic Fatty Liver Disease with Cirrhosis Increases Familial Risk for Advanced Fibrosis. *J. Clin. Invest.* **2017**, *127*, 2697−2704.
(11) Ma, L. L.; Yuan, Y. Y.; Zhao, M.; Zhou, X. R.; Jehangir, T.; Wang, F. Y.; Xi, Y.; Bu, S. Z. Mori Cortex Extract Ameliorates Nonalcoholic Fatty Liver Disease (NAFLD) and Insulin Resistance in High-fat-diet/Streptozotocin-induced Type 2 Diabetes in Rats. *Chin. J. Nat. Med.* **2018**, *16*, 411−417.
(12) Finck, B. N. Targeting Metabolism, Insulin Resistance, and Diabetes to Treat Nonalcoholic Steatohepatitis. *Diabetes* **2018**, *67*, 2485−2493.
(13) Beysen, C.; Schroeder, P.; Wu, E.; Brevard, J.; Ribadeneira, M.; Lu, W.; Dole, K.; O'Reilly, T.; Morrow, L.; Hompesch, M.; Hellerstein, M. K.; Li, K.; Johansson, L.; Kelly, P. F. Inhibition of Fatty Acid Synthase with FT-4101 Safely Reduces Hepatic De Novo Lipogenesis and Steatosis in Obese Subjects with Non-Alcoholic Fatty Liver Disease: Results from two Early-phase Randomized Trials. *Diabetes, Obes. Metab.* **2021**, *23*, 700−710.
(14) Jia, L.; Li, W.; Li, J.; Li, Y.; Song, H.; Luan, Y.; Qi, H.; Ma, L.; Lu, X.; Yang, Y. Lycium Barbarum Polysaccharide Attenuates High-fat diet-induced Hepatic Steatosis by Up-regulating SIRT1 Expression and Deacetylase Activity. *Sci. Rep.* **2016**, *6*, No. 36209.
(15) Li, Y.; Luan, Y.; Li, J.; Song, H.; Li, Y.; Qi, H.; Sun, B.; Zhang, P.; Wu, X.; Liu, X.; Yang, Y.; Tao, W.; Cai, L.; Yang, Z.; Yang, Y. Exosomal miR-199a-5p Promotes Hepatic Lipid Accumulation by Modulating MST1 Expression and Fatty Acid Metabolism. *Hepatol. Int.* **2020**, *14*, 1057−1074.
(16) Yu, F. X.; Zhao, B.; Guan, K. L. Hippo Pathway in Organ Size Control, Tissue Homeostasis, and Cancer. *Cell* **2015**, *163*, 811−828.
(17) Zeng, Q.; Hong, W. The Emerging Role of the Hippo Pathway in Cell Contact Inhibition, Organ Size Control, and Cancer Development in Mammals. *Cancer Cell* **2008**, *13*, 188−192.
(18) Ardestani, A.; Maedler, K. The Hippo Signaling Pathway in Pancreatic β-Cells: Functions and Regulations. *Endocr. Rev.* **2018**, *39*, 21−35.
(19) Geng, C.; Zhang, Y.; Gao, Y.; Tao, W.; Zhang, H.; Liu, X.; Fang, F.; Chang, Y. Mst1 Regulates Hepatic Lipid Metabolism by Inhibiting Sirt1 Ubiquitination in Mice. *Biochem. Biophys. Res. Commun.* **2016**, *471*, 444−449.
(20) Wang, W.; He, Y.; Liu, Q. Parthenolide Plays a Protective Role in the Liver of mice with Metabolic Dysfunction-Associated Fatty Liver Disease through the Activation of the Hippo Pathway. *Mol. Med. Rep.* **2021**, *24*, No. 487.
(21) Ji, S.; Liu, Q.; Zhang, S.; Chen, Q.; Wang, C.; Zhang, W.; Xiao, C.; Li, Y.; Nian, C.; Li, J.; Li, J.; Geng, J.; Hong, L.; Xie, C.; He, Y.; Chen, X.; Li, X.; Yin, Z. Y.; You, H.; Lin, K. H.; Wu, Q.; Yu, C.; Johnson, R. L.; Wang, L.; Chen, L.; Wang, F.; Zhou, D. FGF15 Activates Hippo Signaling to Suppress Bile Acid Metabolism and Liver Tumorigenesis. *Dev. Cell* **2019**, *48*, 460−474.e9.
(22) Nie, J. J.; Liu, Y.; Qi, Y.; Zhang, N.; Yu, B.; Chen, D. F.; Yang, M.; Xu, F. J. Charge-reversal Nanocomolexes-based CRISPR/Cas9 Delivery System for Loss-of-function Oncogene Editing in Hepatocellular Carcinoma. *J. Controlled Release* **2021**, *333*, 362−373.
(23) Zhao, N.; Yan, L.; Zhao, X.; Chen, X.; Li, A.; Zheng, D.; Zhou, X.; Dai, X.; Xu, F. J. Versatile Types of Organic/Inorganic Nanohybrids: From Strategic Design to Biomedical Applications. *Chem. Rev.* **2019**, *119*, 1666−1762.

(24) Nie, J. J.; Qiao, B.; Duan, S.; Xu, C.; Chen, B.; Hao, W.; Yu, B.; Li, Y.; Du, J.; Xu, F. J. Unlockable Nanocomplexes with Self-Accelerating Nucleic Acid Release for Effective Staged Gene Therapy of Cardiovascular Diseases. *Adv. Mater.* **2018**, *30*, No. 1801570.
(25) Foghsgaard, S.; Andreasen, C.; Vedtofte, L.; Andersen, E. S.; Bahne, E.; Strandberg, C.; Buhl, T.; Holst, J. J.; Svare, J. A.; Clausen, T. D.; Mathiesen, E. R.; Damm, P.; Gluud, L. L.; Knop, F. K.; Vilsbøll, T. Nonalcoholic Fatty Liver Disease Is Prevalent in Women With Prior Gestational Diabetes Mellitus and Independently Associated With Insulin Resistance and Waist Circumference. *Diabetes Care* **2017**, *40*, 109−116.
(26) Petersen, M. C.; Madiraju, A. K.; Gassaway, B. M.; Marcel, M.; Nasiri, A. R.; Butrico, G.; Marcucci, M. J.; Zhang, D.; Abulizi, A.; Zhang, X. M.; Philbrick, W.; Hubbard, S. R.; Jurczak, M. J.; Samuel, V. T.; Rinehart, J.; Shulman, G. I. Insulin Receptor Thr1160 Phosphorylation Mediates Lipid-Induced Hepatic Insulin Resistance. *J. Clin. Invest.* **2016**, *126*, 4361−4371.
(27) Smith, G. I.; Shankaran, M.; Yoshino, M.; Schweitzer, G. G.; Chondronikola, M.; Beals, J. W.; Okunade, A. L.; Patterson, B. W.; Nyangau, E.; Field, T.; Sirlin, C. B.; Talukdar, S.; Hellerstein, M. K.; Klein, S. Insulin Resistance Drives Hepatic De Novo Lipogenesis in Nonalcoholic Fatty Liver Disease. *J. Clin. Invest.* **2020**, *130*, 1453−1460.
(28) Eberlé, D.; Hegarty, B.; Bossard, P.; Ferré, P.; Foufelle, F. SREBP Transcription Factors: Master Regulators of Lipid Homeostasis. *Biochimie* **2004**, *86*, 839−848.
(29) Kim, G. H.; Oh, G. S.; Yoon, J.; Lee, G. G.; Lee, K. U.; Kim, S. W. Hepatic TRAP80 Selectively Regulates Lipogenic Activity of Liver X Receptor. *J. Clin. Invest.* **2015**, *125*, 183−193.
(30) Li, Z.; Xu, G.; Qin, Y.; Zhang, C.; Tang, H.; Yin, Y.; Xiang, X.; Li, Y.; Zhao, J.; Mulholland, M.; Zhang, W. Ghrelin Promotes Hepatic Lipogenesis by Activation of mTOR-PPARγ Signaling Pathway. *Proc. Natl. Acad. Sci. U.S.A.* **2014**, *111*, 13163−13168.
(31) Hasenfuss, S. C.; Bakiri, L.; Thomsen, M. K.; Williams, E. G.; Auwerx, J.; Wagner, E. F. Regulation of Steatohepatitis and PPARγ Signaling by Distinct AP-1 Dimers. *Cell Metab.* **2014**, *19*, 84−95.
(32) Dif, N.; Euthine, V.; Gonnet, E.; Laville, M.; Vidal, H.; Lefai, E. Insulin Activates Human Sterol-Regulatory-Element-Binding Protein-1c (SREBP-1c) Promoter through SRE Motifs. *Biochem. J.* **2006**, *400*, 179−188.

https://doi.org/10.1021/acsami.2c05889
ACS Appl. Mater. Interfaces 2022, 14, 34328−34341